The influence of contact surface microstructure on vacuum arc stability and arc voltage

tu/e
Research Report
ISSN 0167-9708
Coden: TEUEDE

Eindhoven
University of Technology
Netherlands

Faculty of Electrical Engineering

The Influence of Contact Surface Microstructure on Vacuum Arc Stability and Arc Voltage

by
FU Yanhong

EUT Report 87-E-186
ISBN 90-6144-186-2
December 1987

Eindhoven University of Technology Research Reports

EINDHOVEN UNIVERSITY OF TECHNOLOGY

Faculty of Electrical Engineering
Eindhoven The Netherlands

ISSN 0167- 9708

Coden: TEUEDE

THE INFLUENCE OF CONTACT SURFACE MICROSTRUCTURE ON VACUUM ARC STABILITY AND ARC VOLTAGE

by

FU Yanhong

EUT Report 87-E-186
ISBN 90-6144-186-2

Eindhoven
December 1987

触头表面粗糙度对真空电弧稳定性的影响

付燕洪

中国西安交通大学留学生

CIP-GEGEVENS KONINKLIJKE BIBLIOTHEEK, DEN HAAG

Fu Yanhong

The influence of contact surface microstructure on vacuum arc stability and arc voltage / by Fu Yanhong. - Eindhoven: Eindhoven University of Technology, Faculty of Electrical Engineering. - Fig. - (EUT report, ISSN 0167-9708; 87-E-186)
Met lit. opg., reg.
ISBN 90-6144-186-2
SISO 661.52 UDC 621.316.57.064.43 NUGI 832
Trefw.: elektrische contacten; boogontladingen.

ABSTRACT

This report shows the results of dc vacuum arc lifetime and arc voltage measurements for contacts with a different surface microstructure, which was realized by treating the contact surface with different roughness emery paper. Large influences of the contact surface microstructure on dc arc lifetime (several tens of times difference at most), arc voltage (30% difference at most) and arc erosion behaviour have been found.The mechanism of the surface microstructure influence on dc arc stability has been analysed and explained preliminarily.

Fu Yanhong
THE INFLUENCE OF CONTACT SURFACE MICROSTRUCTURE ON VACUUM ARC STABILITY AND ARC VOLTAGE.
Faculty of Electrical Engineering, Eindhoven University of Technology, The Netherlands, 1987.
EUT Report 87-E-186

The addres of the author:

Mrs. Fu Yanhong, M.Sc.,
Electrical Energy Systems Group,
Faculty of Electrical Engineering,
Eindhoven University of Technology,
P.O. Box 513,
5600 MB Eindhoven,
The Netherlands

On leave from the Department of Electrical Engineering,
Xián Jiaotong University, The People's Republic of China.

CONTENTS

1. INTRODUCTION

The influence of the contact surface condition on vacuum arc behaviour has been investigated for many years, but it is still considered as a complicated topic. For a given material, the subject has two fields: one is contact surface contamination and impurity, the other is contact surface microstructure.

The influence of surface contamination on vacuum arc has been proved by many experiments in recent years. Especially Jüttner and his coworkers published many papers in this field [1-13]. They consider that a contaminated surface coincides with longer dc arc lifetime, smaller cathode crater size, larger cathode erosion area, lower cathode erosion rate, lower arc voltage and lower cathode spot current density. Other authors [14,15] measured the velocity of cathode spot decreased when contact surface becomes more clean. That the arc itself is an effective methode for cleaning cathode surface has also been found. A statement has been formulated[16]: on the contaminated contact surface there is mainly one kind of cathode spot with the characteristics of fast moving and weak erosion(so called type I spots); on the clean contact surface there is mainly another kind of cathode spot with the characteristics of slow moving and strong erosion(so called typeII spots).

Only few papers deal with the relation between arc behaviour and surface microstructure. Some authors think the effect of surface microstructure is not important[15,17]. Daalder[18] has shown the arc voltage has different values on polished(19 V), half polished(17 V) and roughened(16-17 V) copper contacts. Sethuraman[19] found that the direction of cathode spot motion is affected by cathode surface scratches, and that smaller craters appear on more rough surfaces. Ecker[20] proposed two theoretical

models for cathode spots: spots on smooth surface and spots on rough surface(with average structural microroughness and with individual structural roughness). But these models have not been checked by experimental work.

Since it is well known that the smoother the cathode surface is the higher the breakdown voltage is, the vacuum circuit breaker manufacturer usually makes the contact surface as smooth as possible. But it is doubtful that the vacuum interrupter with the more smooth contact surface has the better characteristics of current interrupting. Therefore it is worth to study the influence of the degree of surface roughness on the current interrupting characteristics, such as the arc stability (directly related with current chopping), arc erosion, etc..

2. EXPERIMENTAL CIRCUIT

The experimental circuit is shown in Fig.2.1. The DC supply consists of six 12V batteries. (The total voltage is 72 V.) The master switch (MS) is for safety reasons. It limits the maximum time of current flow. Its closing duration is normally 100 ms. The variable carbon moulded resistor (R) is used for adjusting the arc current. The circuit inherent inductance (L) and parastic capacitance (C) are about 20 μH and 400 pF respectively. The arc current is measured by means of a shunt (R_s). The vacuum interrupter (VB) has been degassed and baked out for at least 16 hours with the maximum temperature of 400 $^{\circ}$C before measurement. The pressure inside the interrupter is in the order of 10^{-6} Pa. The average contact opening speed is about 2 m/s. The final distance between two contacts is 5 mm.

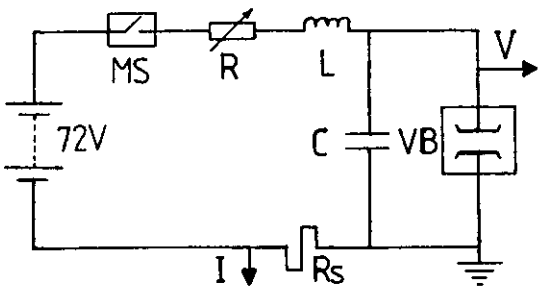

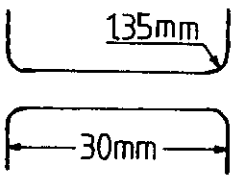

Fig.2.1 *Experimental circuit.* Fig.2.2 *Contact configuration.*

The contacts which has been used are made of OFHC copper. Their configuration is shown in Fig.2.2. The diameter of each contact is 30 mm. The edge curvature radius is 1.35 mm. The contacts are in parallel and the edges are rounded to uniform the electric field in the vacuum gap. Before the interrupter is assembled, the contacts have been etched in acid liquid for at least 5 mins.

The contact surface roughness has been influenced by treating with different emery papers (No.P.220, P.400 and P.800., these numbers mean there are 220, 400 and 800 silicon particles in 1 mm^2.) and a rotating polishing disk (grain size 1 μm). The electric field enhancement factor β is taken as a measure for the degree of contact surface roughness. The gap distance(d) was 0.25 mm. The emission current was limited at lower than 500 μA. The max. voltage over the gap was 5–10 KV which depends on the emission current. The Fowler-Nordheim plot is the curve of $\mathrm{Log}_{10}[I/(\frac{V}{d})^2]$ as a function of (d/V). β can be obtained from the FN plots.* It is found that the value of β is larger for the contact surface treated with rougher emery paper. For instance, β is roughly 800, 600 and 400 for the surface treated with P.220, P.400 and P.800 emery paper respectively; and β is about 200 for the surface treated with a rotating polishing disk.

---

* $\beta = \frac{6.831\times10^9\ \varphi^{3/2}}{2.303\times(-\mathrm{tg}\alpha)}$, φ is the work function of cathode material, $\mathrm{tg}\alpha$ is the slope of FN curve[21].

3. DETECTION OF THE CONTACT PRODUCTS EMITTED BY ARCS

The residual gas content in the interrupter and the products emitted by the arc from surfaces with different microstructure were determined by mass spectrum analysis using a Balzers QMG 311 Quadrupole mass spectrometer. It is mounted on the vacuum interrupter as shown in Fig.3.1.

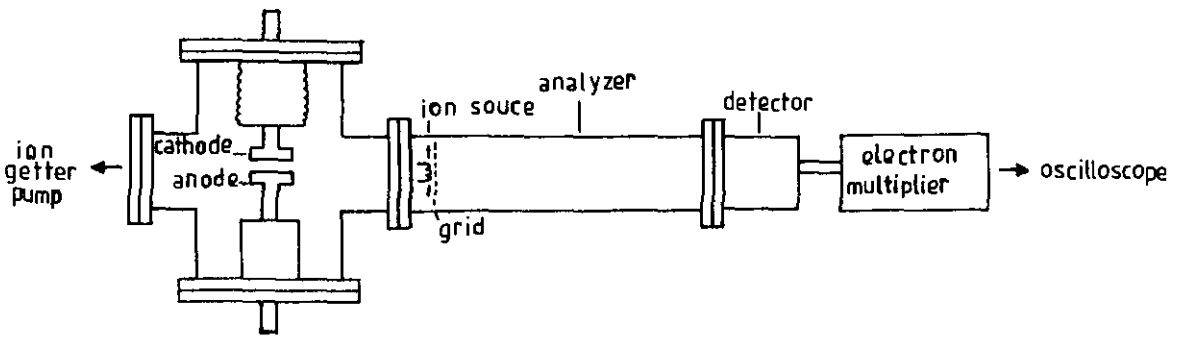

Fig.3.1 *Schematic diagram of vacuum interrupter and mass analyzer.*

1) Residual gases analysis

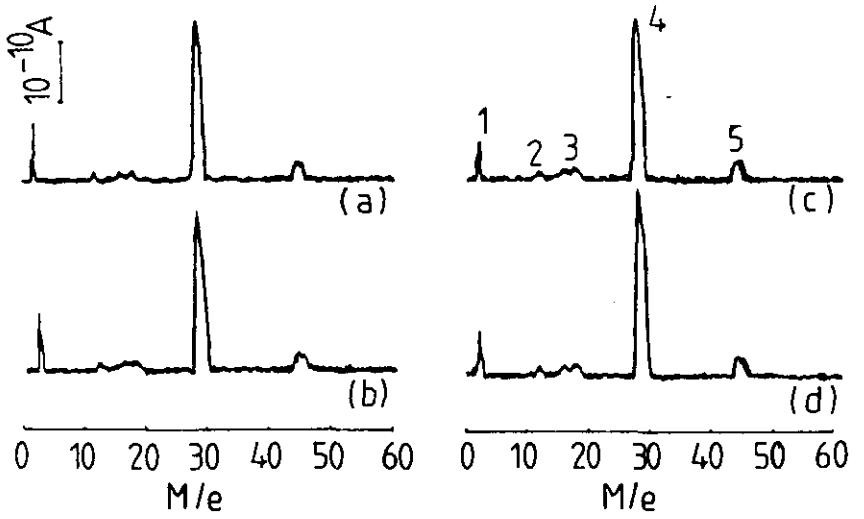

Fig.3.2 *The residual gas signal from the interrupter. The contact surface was treated respectively with emery paper* P.220 (a); P.400 (b); P.800 (c); *and a rotating polishing disk* (d). *Possible ions are*: 1) H_2^+; 2) C^+; 3) CH_n^+, H_2O^+; 4) CO^+, N_2^+; 5) CO_2^+.

Before the ion source was applied, the pressure inside the interrupter was lower than 1×10^{-5} Pa. When the ion source was fed by a 0.1 mA emission current, the pressure rose more than two time orders caused by filament heating. After the pressure had been decreased gradually by the ion getter pump, the ion source could be fed by a larger emission current up to 1 mA and the pressure could be lower than 1×10^{-4} Pa. Fig.3.2 shows the residual gas signal of four interrupters with different surface roughness. The signals were all enhanced by a electron multiplier with a damping frequency of 300 Hz. One can see, there is no significant difference in the amounts of the various ions from the four interrupters, except mass 28 (CO or N_2) in (d) is 18% higher than in others. It is therefore obvious, that the residual

2) The products from the contact surface emitted by the arc.

As described above, the different degree of contact surface roughness is achieved by treatment with different emery paper or rotating polishing disk. The grinding material of the emery paper is silicon carbide (SiC). The polishing material of the rotating polishing disk is a diamond compound. Although all contacts have been well cleaned and baked out after the mechanical treatment, it could happen that some particles, which were pressed in the contact surface layer from the polishing material, were still there. These particles are one kind of the surface contamination. When an arc is drawn between contacts, these impurity particles will be heated by cathode spots and will be evaporated together with copper.

The interesting point is the amount of impurity ions coming from surfaces with different degree of roughness during the arcing. This work has to be done very carefully to avoid influencing surface roughness and condition surface by doing measurements. The arc current must not be too large, otherwise it would erode the contact strongly; and it must not be too small, otherwise the lifetime is too short, the measurements can not be performed. The number of measurements should also be limited for the same reason.

Fig.3.3 shows the ion current spectrum during arcing. The copper ions have been found with the amplitude of the order of 10^{-8} A. The neutral particles from the arc can also be detected after they have been ionized by electron bombardment in the ion souce. For instance in Fig.3.4.

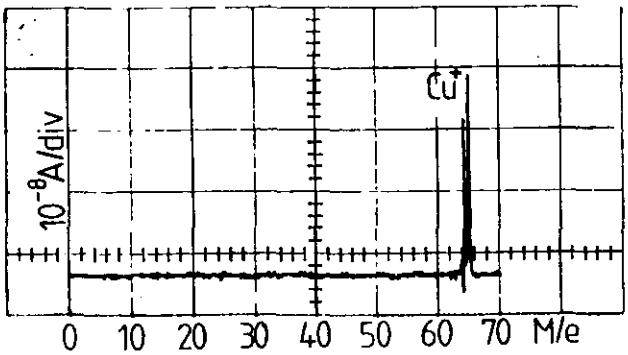

Fig.3.3 *Mass spectrum of the copper ions directly from the arc of 16* A. *Contact surface was treated with* P.220 *emery paper.*

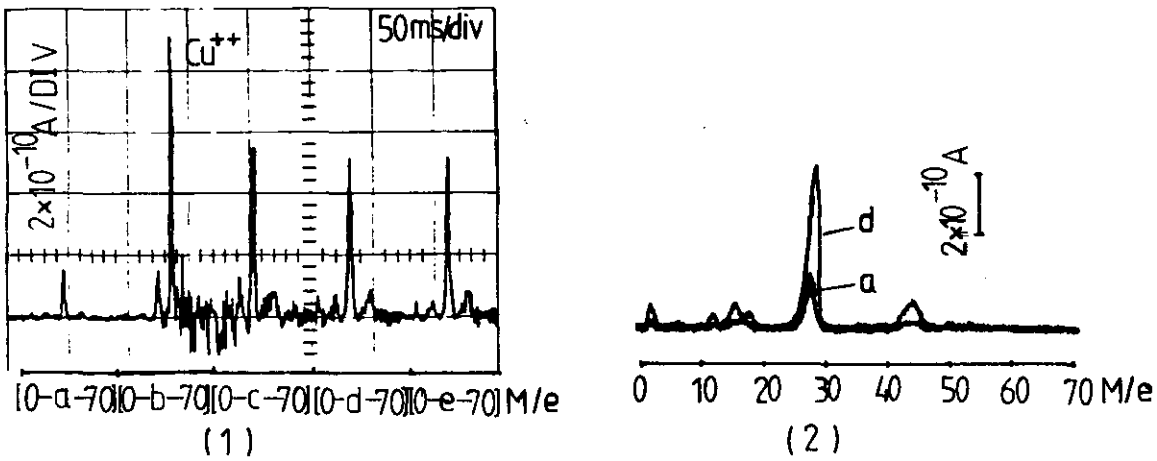

Fig.3.4 *Mass spectrum of the ions ionized from neutral yield before(include copper), during and after an arc of 16* A. *The contact surface was treated with* P.220 *emery paper. The mass scan speed was 1* (M/e)/ms. (1) *repeated mass detection for each cycle:* M/e = 0-70; (2) *enlargement of first cycle (curve* a: *before arc) and fourth cycle (curve* d: *after arc) from* (1).

Fig.3.4(1) shows the repeated mass spectrum of the ions with mass number from 0 to 70. The first cycle (a) was before arc ignition. The second cycle (b) was during arcing. The arc lifetime was about 10 ms which is much smaller than one cycle of mass scan (70

ms). Therefore during one arcing only one kind of copper ions could be detected which can be Cu^{+}, or Cu^{++}, Cu^{3+}, Cu^{4+} like Cu^{++} in cycle (b). The noise signal between the second cycle and the third cycle was vibration noise of the contact movement. The third (c)(after 70ms), fourth (d)(after 140ms) and fifth (e)(after 210ms) cycle were after the arc extinction. It is clearly shown in Fig.3.4(2) that the number of impurity ions were increased by arcing. The largest yields were at mass number 28. They could be the ions of CO or N_2, Si from the cathode surface.

Fig.3.5 shows the relative percentage of impurity ion current increased by arcing. The arc current was 16 A. The data are the average values of the first five measurements. The ion current before and after arc is defined as the peak height as in Fig.3.4(2).

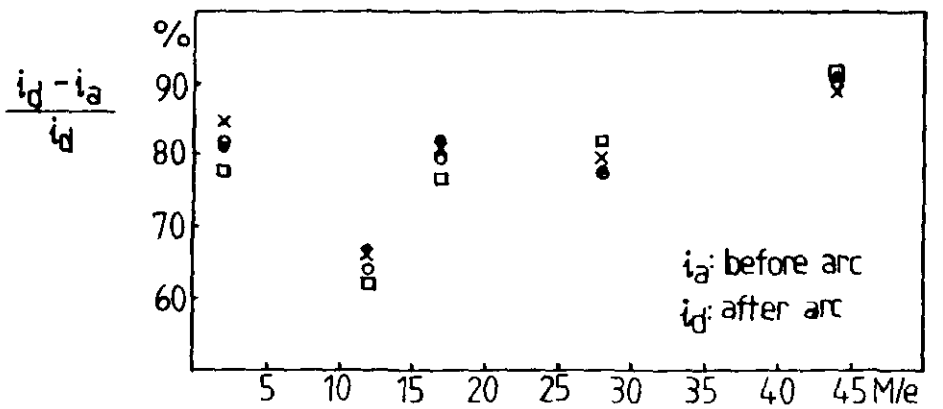

Fig 3.5 The relative percentage of impurity ion current increased by arcing."□": the surface polished with the rotating polishing disk."•","x", and "o": the surfaces treated with the emery paper No.P.220, P.400, and P.800 respectively.

One can see in Fig.3.5, that the impurity ion currents increased by arcing are nearly the same on four surfaces with different degree of roughness. But the max. impurity yield, increased by

arcing, is about 2% of the arc produced copper ion yield(see Fig.3.4 and Fig.3.3.). Therefore the contacts with the different degree of surface roughness have nearly the same degree of surface contamination in our experiments.

4. A CHECK OF THE DEPENDENCE OF MEASUREMENT DATA TO CONTACT CLEANING PROCEDURE.

In the last section, the arc emitted impurity yield from the contact surface has been detected. Now, in order to check the respondency of measurement data to the effect of our contact cleaning procedure, a comparison has been done between two groups of experiments. The first group of experiments were done by using a contact which was just processed by drawing a large number of arcs with in total about 500 C transferred charge. The second group of experiments were done by using a contact which was first processed by about 500 C arcs, secondly exposed in air for 132 hours, then cleaned and baked out by the same procedure as described in section 2. The difference is then the degree of contamination, not the microstructure.

The arc lifetime τ is defined as in Fig.4.1. The average arc lifetime $\bar{\tau}$ is the arithmetic mean of a number of measured τ values. It is known that the arc voltage consists of a certain dc level and an superimposed high frequency component. They are defined in Fig.4.2. The average arc lifetime $\bar{\tau}$, arc voltage DC level and high frequency peak number per millisecond have been measured. The maximum relative deviation of the data between two groups is respectively 0.14 for average arc lifetime, 0.03 for arc voltage DC level, and 0.21 for arc voltage HF peak number per ms. These relative deviations are all similar to their own standard deviation of the measurement data. Therefore the

difference between two groups of data is negligible. The cleaning procedure is satisfactory. But one point has to be noted: the above comparison is only a check for the contact surface oxide layer. A similar check for contacts contaminated by emery paper is almost impossible.

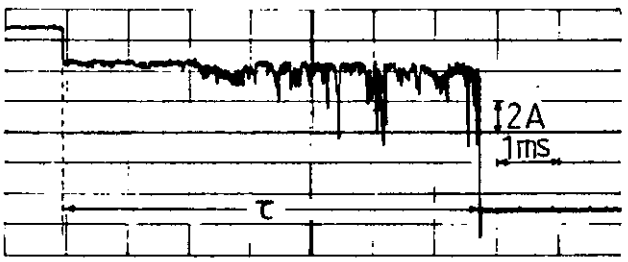

Fig.4.1 *Arc current oscillogram.*

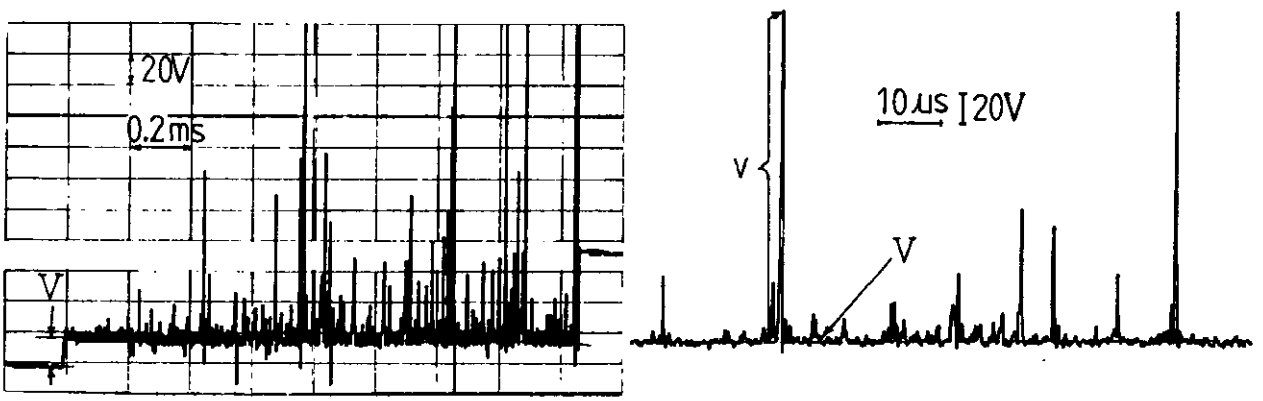

Fig.4.2 *The arc voltage oscillogram.* V *is* DC *component,* v *is* HF *component.*
(a) *whole signal;* (b) *enlarged part.*

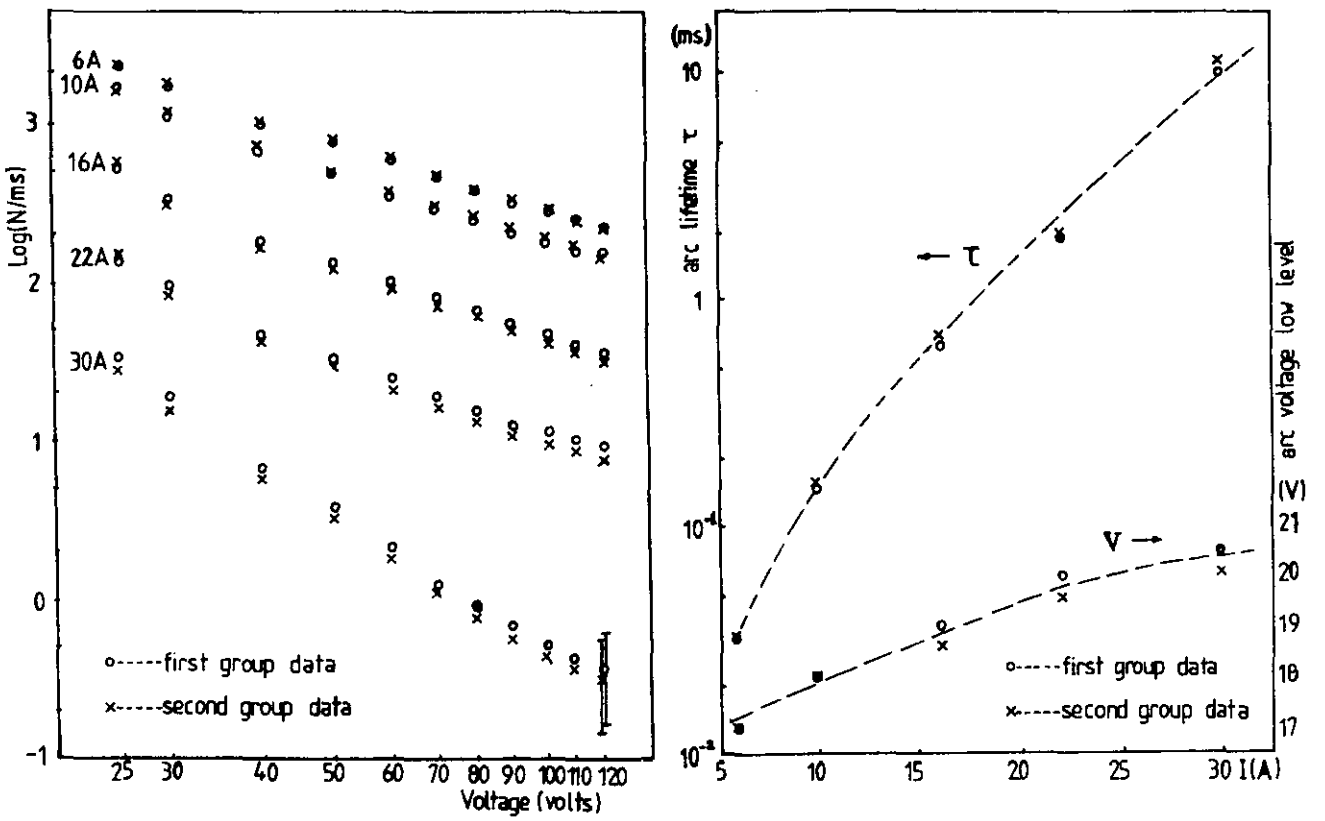

Fig.4.3 *Number of high frequency arc voltage peaks as function of voltage.*

Fig.4.4 *Arc average dc lifetime and arc voltage dc level as function of arc current.*

5. THE DC ARC LIFETIME MEASUREMENT.

In many years of research, it is known, that the dc arc lifetime is directly related to arc stability. There are many factors affecting the arc stability[22, 23]. This section only focuses on the influence of contact surface microstructure on DC arc lifetime.

Four contacts have been used: "roughened" contact was treated with emery paper P220; "normal" contact was treated with emery paper P800; "smooth" contact was polished by a rotating polishing disk with diamont compound and was conditioned by high voltage (the electric field enhancement factor β was about 100); "eroded" contact was processed by dc arc with the total transferred charge of 540 C. About 80% of contact surface has been covered by arc traces. The cleaning and baking out procedure of all contacts were the same as described in section 2. The experimental circuit and the configuration of the contact were the same as shown in Fig.2.1 and Fig.2.2. The arc lifetime τ is defined the same as in Fig.4.1. The average arc lifetime $\bar{\tau}$ is the arithmetic mean of twenty five measured values. The experiments were carried out from low current to high current for keeping the same primary surface condition as much as possible. The results are shown in Fig.5.1.

It can be seen, that the arc lifetime for the "roughened" contact is longer than the arc lifetime for the "normal" contact. The arc lifetime for the "smooth" contact is shorter than that for the "normal" contact and almost the same as that for the arc eroded contact. It might be explained by the more scratches and protrusions on the rough contact and higher field enhancement at those locations. The cathode spots can jump easily among these scratches and protrusions, therefore arc can sustain a longer time. Sethuraman also found the motion of cathode spot controlled by the surface scratches[19].

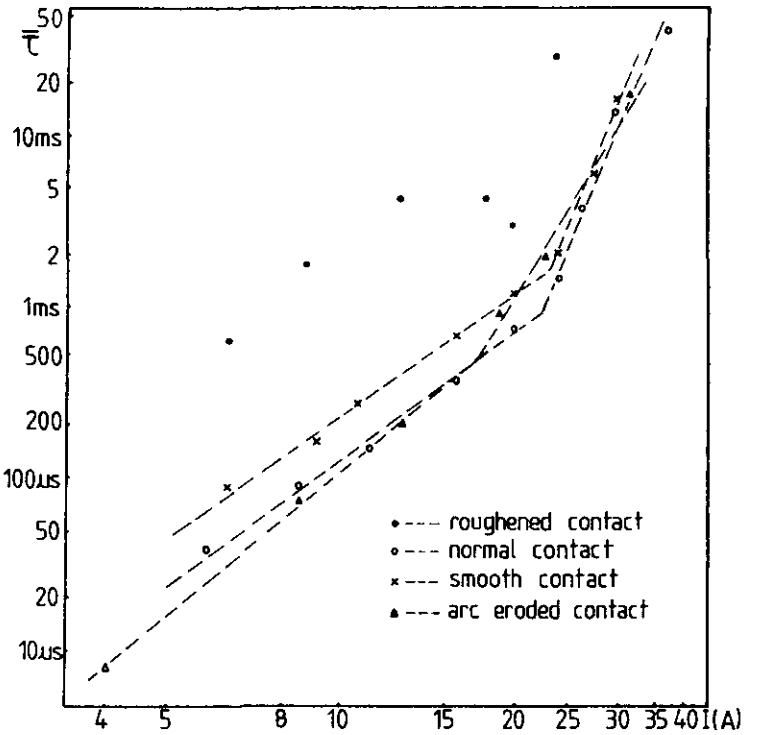

Fig.5.1 *Average arc lifetime versus arc current.*

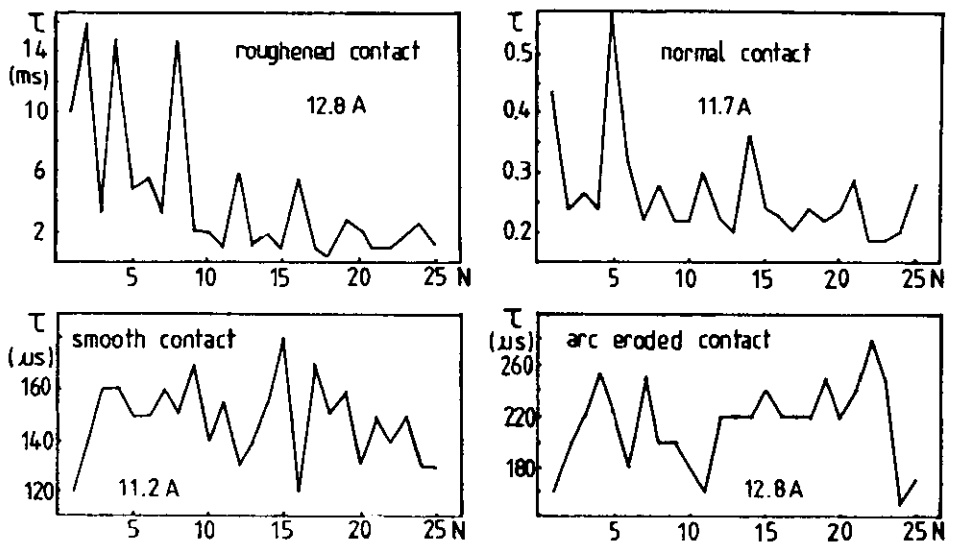

Fig.5.2 *The typical distribution of four contacts.*
τ is the arc lifetime.
N *is the number of the measurement.*

The arc lifetime has some variations during lifetime measurement as can be seen from the distribution of the arc lifetime as shown in Fig.5.2. There is an apparent decrease of lifetime during measurement on the "roughened" contact and also on the "normal" contact. But there is not such a tendency on the "smooth" contact and on the "arc eroded" contact, the lifetimes are rather stable in both cases. From this point of view, the arc itself has a tendency to "smooth" a contact surface. This might be the reason of the almost same arc lifetime on arc eroded contact and on smooth contact.

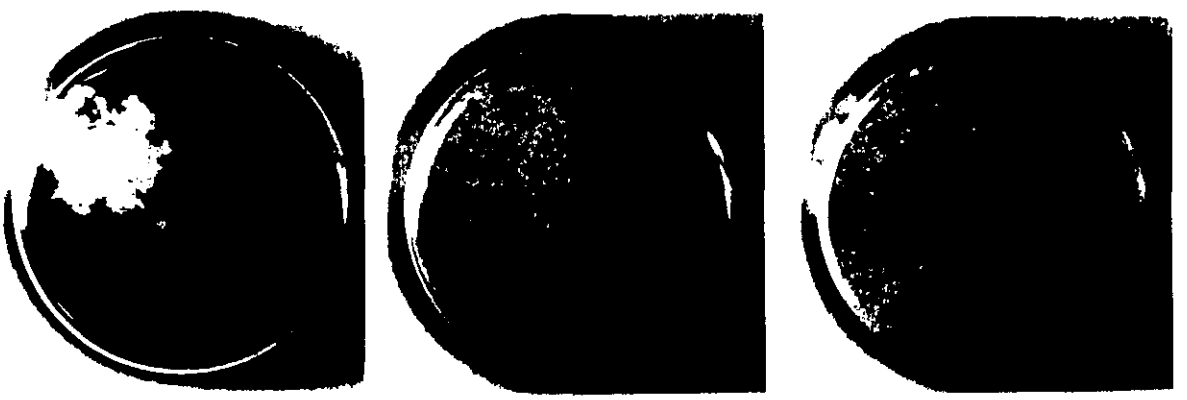

Fig.5.3 *The contact surface after arc lifetime measurement.*
(a) *smooth contact;* (b) *normal contact;*
(c) *roughened contact.*

The different erosion areas on surfaces of different roughness have been observed. They are shown in Fig.5.3. The total transferred charges were respectively 50 C for smooth contact; 34 C for normal contact and 32 C for roughened contact. The erosion area has been estimated as 15% for smooth contact, 30% for normal contact and 60% for roughened contact. It can be clearly seen, that the erosion area on the smooth contact was small. The craters overlapped. The erosion area on the roughened contact was diffused to a large part of contact surface. The craters were

more individual, and the crater size was smaller than on the smooth contact. The situation on the normal contact was in between the smooth contact and the roughened contact. The erosion behaviour on the rough surface has the characteristics of "type I" cathode spot; the erosion behaviour on the smooth surface has the characteristics of "type II" cathode spot. This means that at a certain degree of surface contamination, the different degree of surface roughness may also causes the different "type" of cathode spot.

6. THE ARC VOLTAGE MEASUREMENTS.

The arc voltage, as well known, is strongly dependent upon the cathode material. Arc voltage dependency on electrode diameter, electrode gap, and axial magnetic field etc. has also been found[21]. Here only the influence of contact surface microstructure will be studied for the cathode material copper. A typical arc voltage oscillogram is shown in Fig.4.2.

1) Arc voltage dc component.

Fig.6.1 shows volts-ampere characteristics of the arc from five contacts with different degree of roughness. Again the four contacts which are "roughened", "normal", "smooth" and "arc eroded" have been used. Besides, a "very rough" contact which was treated with emery paper No.P.60 also has been used.

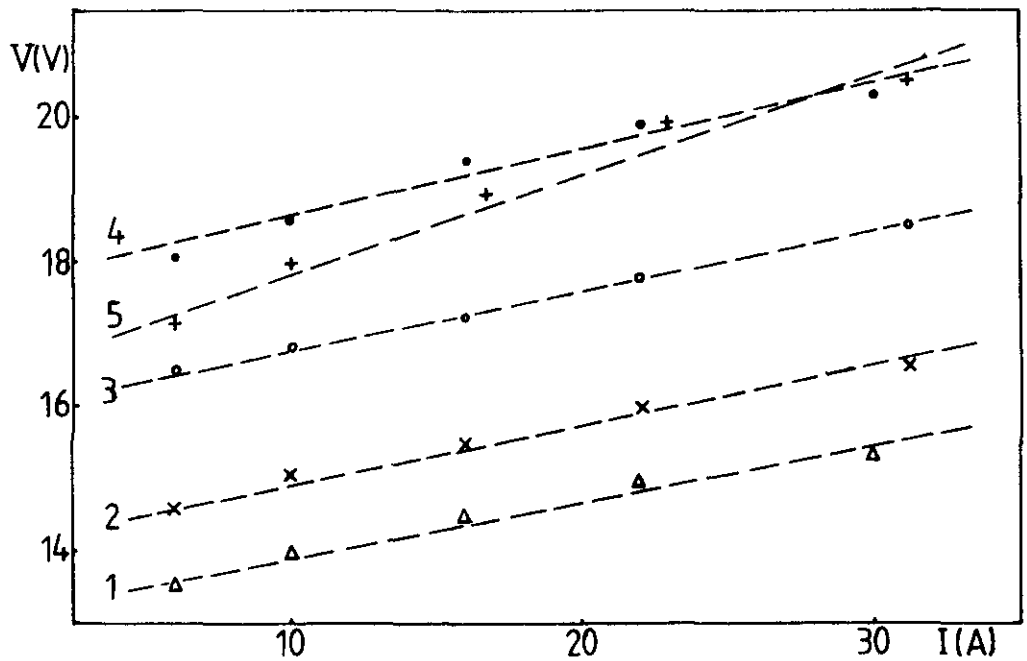

Fig.6.1 *The arc voltage* DC *component as function of the arc current.* 1—*very rough contact;* 2—*roughened contact;* 3—*normal contact;* 4—*smooth contact;* 5—*arc eroded contact.*

The slopes dV/dI for four different contacts are approximately the same. A higher dV/dI appears only on the arc eroded contact. The arc voltage at a given current is higher for smoother surface. The difference of more than 4 V between smooth surface and very rough surface is remarkable. The arc voltage of the arc eroded contact is near to that of the smooth contact. Detailed measurements, of the variation of the V-I characteristic for roughened contacts after charge transfer are shown in Fig.6.2. The arc voltage for roughened contact increased with the increase of transferred charge. The increasing of arc voltage was fast in the first 100 C of transferred charge.

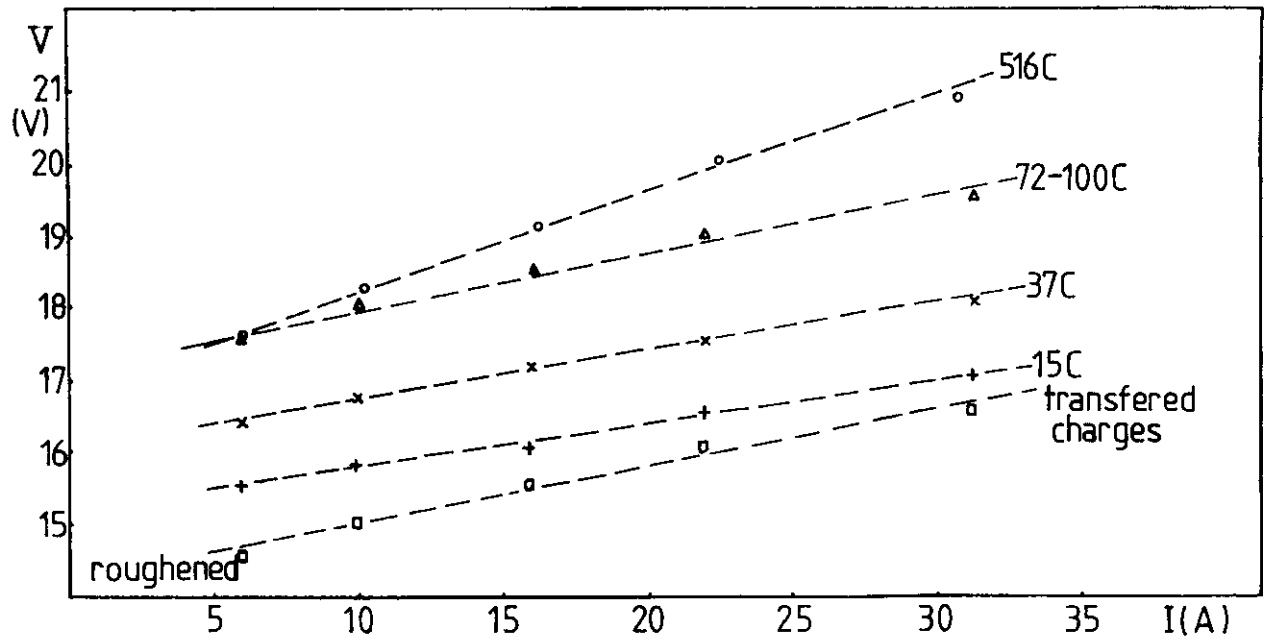

Fig.6.2 V-I *characteristics for roughened contact varies with the transferred charge. Q is the transferred charge for eroding the surface.*

2) Arc voltage high frequency component.

Fig.6.3 shows the typical arc voltage and arc current oscillograms for the contacts with different degree of roughness. It has been noticed[22], that an arc voltage high frequency peak always coincides with an arc current instability dip. The higher the HF peak is, the deeper the current dip is. The measurements of the number of arc voltage HF peaks as a function of the voltage level for some arc currents and some contact surface microstructures, are shown in Fig.6.4. The contacts used were: "roughened", "smooth" and "arc eroded". It is clear, that the arc voltage HF components are higher and more frequent for a lower arc current at a given contact surface microstructure and they are also higher and more frequent for a smoother surface at a given arc current. The strongly eroded surface shows similar

behaviour as the smoother surface.
The arc voltage (both dc and HF component) is very sensitive to surface microstructure.

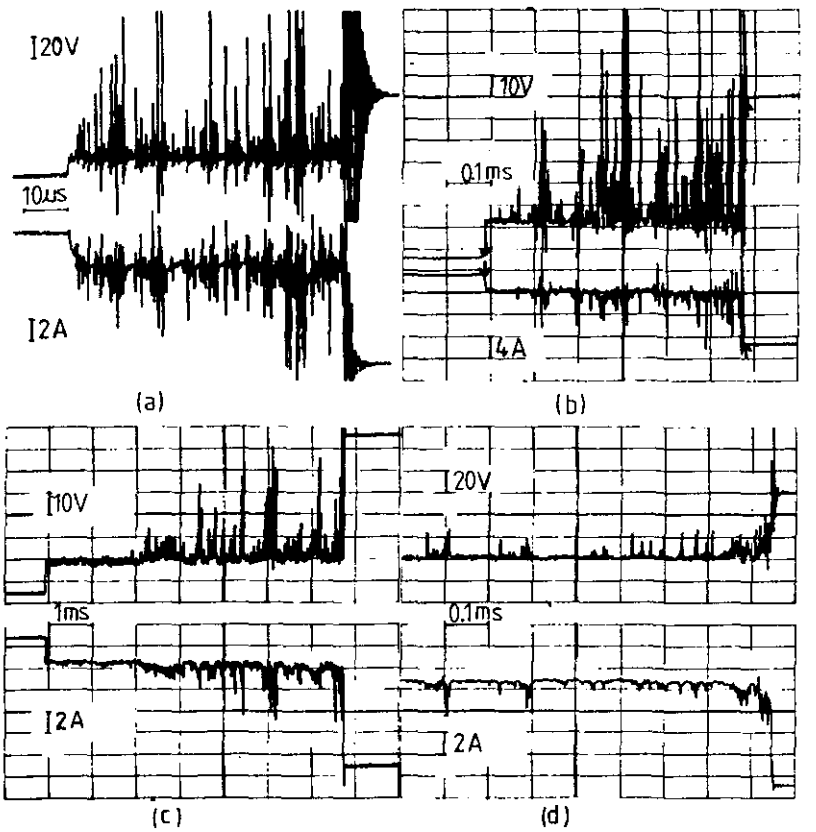

Fig.6.3 *Oscillograms of arc voltage and arc current for some contact surface microstructures. Current is* **18 A** *for all four cases.* (a) "*smooth*" *contact*; (b) P800 *contact*; (c) P400 *contact*; (d) P220 *contact*.

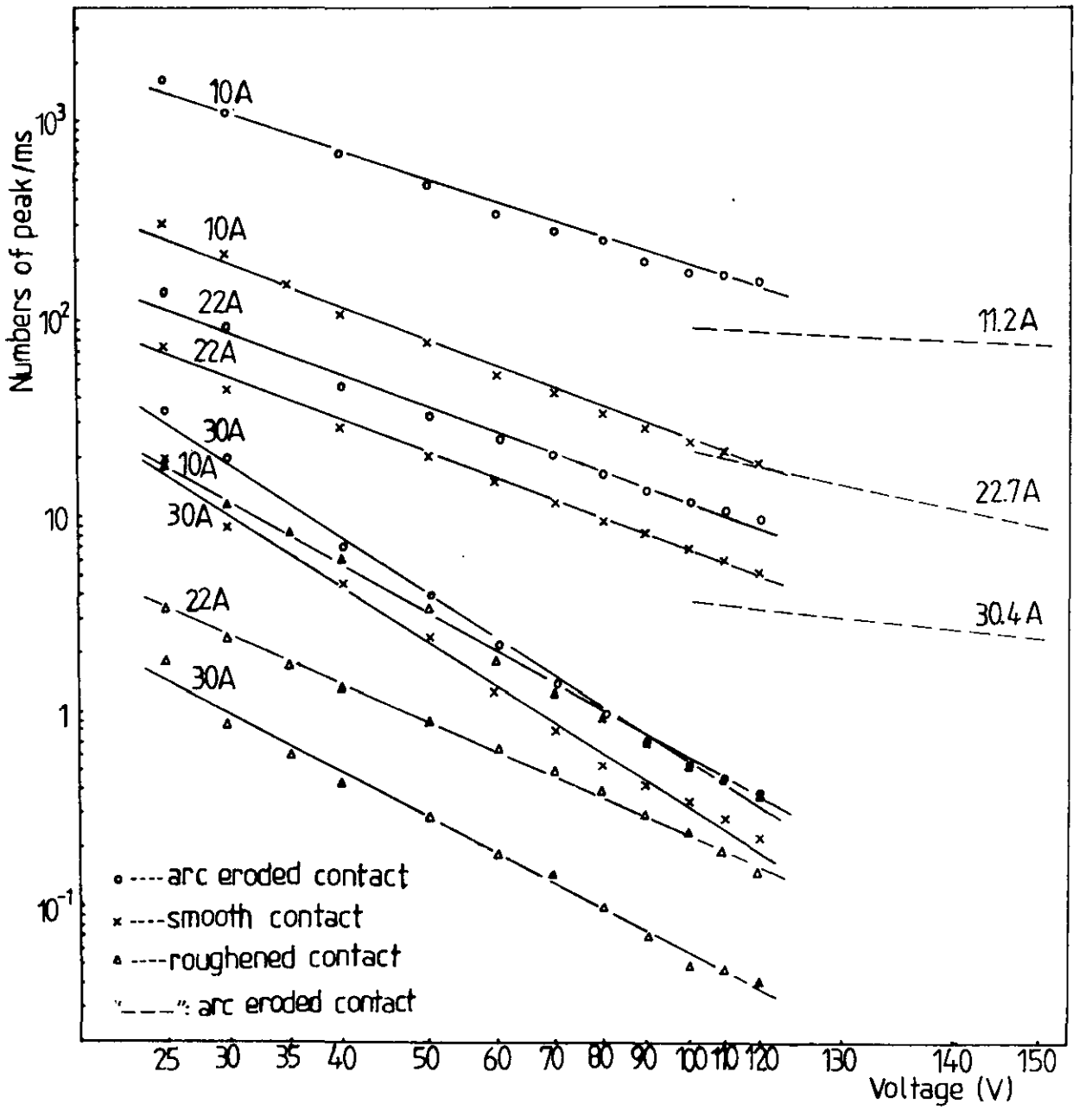

Fig.6.4 *Numbers of arc voltage high frequency peaks as a function of voltage level with some arc currents and contact surfaces. The dotted line is measured by Smeets* [22].

7. ANALYSIS AND DISCUSSION.

The results of measurements on arc lifetime and arc voltage have been shown in the previous part of this report. The apparent influences of the contact surface roughness on arc lifetime, arc voltage and arc erosion behaviour have been comfirmed. The explanation of these phenomena is, however, complicated. A preliminary attempt on the arc stability and erosion behaviour is given in this section.

In order to simplify analysis, a single protrusion model will be used for simulating the arc erosion on the contact surface with a certain degree of roughness. Next presumptions have been made for a model, based on the work of Daalder[23]: (a) the constructure shape of protrusion is a coniform with a conical angle (θ) and a height (ℓ); (b) the direction of current flowing is homogeneously parallel to the radius of erosion layer into the cathode; (c) the erosion layer is a part of a spherical surface with radius r and conical angle θ. This model includes Daalder's model when θ is 180°. It is shown in Fig.7.1. r_a is the radius of a crater. When θ is 180°, r_a is r.

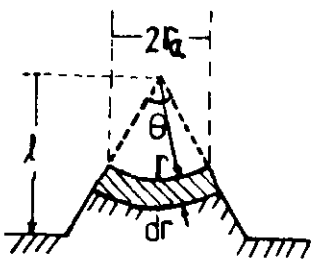

Fig.7.1 *Surface microstructure included calculation model for arc erosion.*

Considering the whole heat transfering procedure as adiabatic heating, the energy balance of the layer dr can be expressed

as[23]:

$$I_e^2 \cdot \frac{\rho(T)}{A} = A\, m_s c_p \frac{\partial T}{\partial t} \qquad (1)$$

$$I_e = 0.9 \cdot I$$

$$A = r^2 \int d\Omega = 4\pi r^2 \sin^2 \frac{\theta}{4}, \quad r \leq \frac{\ell}{\cos(\theta/2)}$$

where m_s is density of cathode material, I_e is electron current at cathode, c_p is specific heat of the solid metal. $\rho(T)$ is temperature dependent electric resistivity, according to the law of Wiedemann-Franz-Lorenz: $\rho(T)=LT/\lambda$. L is the Lorenz constant. λ is the thermal conductivity, and is more or less a constant (λ_o) in solid state. At fusion point λ changes approximately 1/2. Therefore the time to remove cathode metal mass from the protrusion or to form a crater is:

$$t(\theta) = \frac{16\pi^2 r^4 m_s \lambda_o \sin^4 \frac{\theta}{4}}{I_e^2 L} \left[\int_{T_o}^{T_s} c_p \frac{dT}{T} + \frac{P_s}{2T_s} \right] \qquad (2)$$

when $\theta = 180^\circ$, then:

$$t(180) = \frac{4\pi^2 r'^4 m_s \lambda_o}{I_e^2 L} \left[\int_{T_o}^{T_s} c_p \frac{dT}{T} + \frac{P_s}{2T_s} \right] \qquad (3)$$

where T_o is the room temperature, T_s is the melting temperature, and P_s is the heat of melting. The radius of a crater for a given

current is:

$$r_a(\theta) = r(\theta)\cdot\sin\frac{\theta}{2} = K_1 \cos\frac{\theta}{4} (I^2t)^{1/4} \qquad (4)$$

$$\text{so} \quad r_a(180) = r(180) = K_1 \frac{1}{2}\cdot\sqrt{2}\ (I^2t)^{1/4} \qquad (5)$$

Here $K_1 = \{ L/[\pi^2 m_s \lambda_o (\int_{T_o}^{T_s} c_p \frac{dT}{T} + \frac{p_s}{2T_s})] \}^{1/4}$; for copper $K_1 = 2.88\cdot10^{-5}$ m/$(A^2s)^{1/4}$.

The mass removed from the cathode into plasma is :

$$M(\theta) = m_s v = m_s \int_0^r A\cdot dr = m_s \frac{4}{3}\pi r^3 \sin^2\frac{\theta}{4} = \frac{K_2 (I^2t)^{3/4}}{\sin(\theta/4)} \qquad (6)$$

$$\text{so} \quad M(180) = K_2 \sqrt{2}\ (I^2t)^{3/4} \qquad (7)$$

Here $K_2 = \frac{m_s \pi K_1^3}{48}$; for copper $K_2 = 1.11\cdot10^{-10}$ Kg/$(A^2s)^{3/4}$.

The removed metal mass per unit time (erosion speed) is:

$$(\frac{dM}{dt})_\theta = \frac{K_3 (I^2/t)^{3/4}}{\sin(\theta/4)} \qquad (8)$$

$$(\frac{dM}{dt})_{180} = K_3 \sqrt{2}\ (I^2/t)^{3/4} \qquad (9)$$

Here $K_3 = \frac{3}{4} K_2$; for copper $K_3 = 0.84\cdot10^{-10}$ Kg/$(A^2s)^{3/4}$.

Fig.7.2 shows the ratios of eroion times for constant erosion depth r and erosion depth, mass and speed for constant erosion time, all as function of the conical angle θ. All quantitives are related to their equivalent for a flat surface surface (θ = 180°).

It can be seen clearly that, (a). at a given current and time, the depth (r), the mass (M) and speed (dM/dt) of erosion for a protrusion on the rough cathode are higher a factor of $1/[\sqrt{2}\cdot\sin\frac{\theta}{4}]$ than for a crater on the flat cathode; (b). at a given current and erosion depth, the time (t) to vaporize the cathode metal for a protrusion on the rough cathode is shorter a factor of $4\cdot\sin^4\frac{\theta}{4}$ than for a crater on the flat cathode, the radius and depth of a crater for a protrusion is smaller a factor of $\sin\frac{\theta}{2}$ and $[1 - \cos\frac{\theta}{2}]$ respectively than for a flat cathode respectively; (c). these increasing and decreasing factors are all conical angle dependent, the factors are more sensitive when θ is smaller.

By involving the comparison of the electric field enhancement between a smooth cathode and a rough cathode in Fig.7.3, the results of the experiments in section 5 can be explained as follows: In case of a rough cathode surface, in the neighbourhood of a certain spot emission area, there exists some protrusions where the local field is higher than the breakdown field. The field emission occurs easily on these protrusions. Once a emission area is formed on a protrusion, this protrusion would be melted in short time depending on eq.(2). The crater size is small depending on eq.(4), since there are many protrusions which brings many possibilities to form new spot emission. The spot could often move from one protrusion to another. The distance among craters can thus be somewhat big. Besides eq.(8) shows the erosion speed for a protrusion is larger, this means with less energy for eroding one unit mass, and it could facilitate to sustain arc and to stabilize arc. Therefore the arc lifetime can be long, the craters could be more and arc can be stable.
The analysis on arc voltage influenced by contact surface microstructure is being continued.

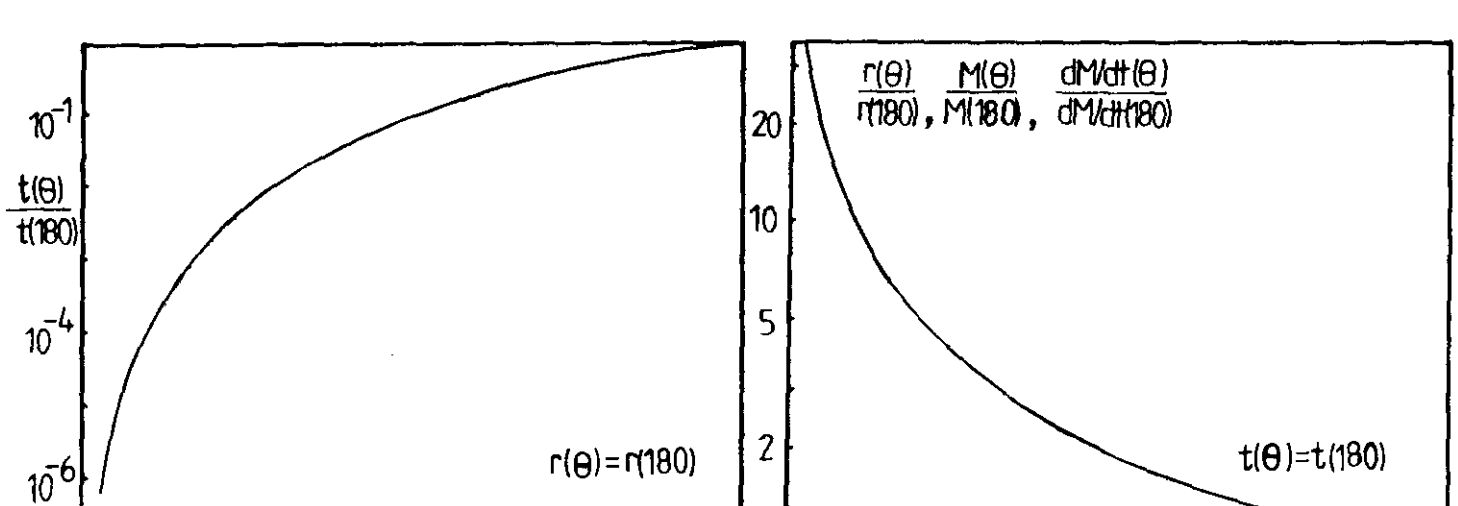

Fig.7.2 *Ratios of the erosion time, the erosion depth, the mass and mass flow for a protrusion and a flat cathode as a function of the conical angle θ.*

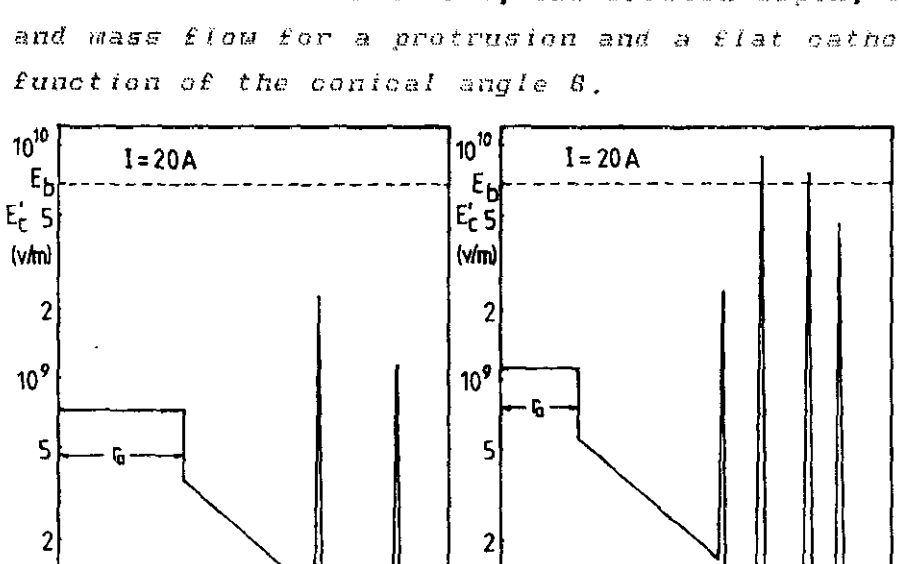

Fig.7.3 *Electric field near crater. (refer to* [22]) (a) *smooth surface;* (b) *rough surface.* E_b: *breakdown field. The dimensions of protrusions are not to scale.*

8. CONCLUSIONS.

- By mass spectrum analysis, it is found that the treatment with different emery paper on a contact surface does not significantly influence the degree of surface contamination.
- The rougher the contact surface is; the longer arc lifetime is, and the more stable the arc is. The arc itself has a tendency to "smooth" the contact surface and therefore to reduce the arc lifetime. The erosion on rougher surface is weaker (smaller crater size), and the distances between the craters on rougher surface are somewhat larger.
- The rougher the contact surface is, the lower arc voltage is (both dc and HF components). The arc erosion itself has an increasing influence on the arc voltage.
- A conic protrusion model for the calculation of Joule heating has been used. The mass flow per Coulomb(for a given current) to the plasma from a conically shaped protrusion (on the cathode) is always larger than from a flat cathode. The more tapered the protrusion is, the larger the difference is. By involving the electric field enhancement on the cathode, the longer lifetime and the weaker erosion on the rougher surface could be explained.
- It is possible that the type I cathode spots (fast moving, weak erosion) coincides not only with the surface contamination but also with the degree of surface roughness.

9. ACKNOWLEDGEMENT.

The author gratefully acknowledges Prof. Dr. W.M.C. van den Heuvel and Dr. R.P.P. Smeets for their advice and valuable discussions. The author wishes to thank Mr. A. van Staalduinen, Mr. P.N. Klijn, Mr. L.A.H. Wilmes and Mr. J.W.G.L. Vossen for their technical help.

10. REFERENCES

[1] Jüttner, B. and E. Freund
Über die Lebensdauer von elektrischen Gleichstrombögen im Ultrahochvakuum.
Beitr. Plasma Phys., Vol. 15(1975), p. 47-61.

[2] Achtert, J. and B. Altrichter, B. Jüttner, P. Pech, H. Pursch, H.-D. Reiner, W. Rohrbeck, P. Siemroth, H. Wolff
Influence of surface contaminations on cathode processes of vacuum discharges.
Beitr. Plasma Phys., Vol. 17(1977), p. 419-431.

[3] Jüttner, B.
Erosion craters and arc cathode spots in vacuum.
Beitr. Plasma Phys., Vol. 19(1979), p. 25-48.

[4] Jüttner, B.
Erosion phenomena on contaminated cathodes caused by electrical discharges in ultra high vacuum.
Beitr. Plasma Phys., Vol. 18(1978), p. 265-269.

[5] Guile, A.E. and B. Jüttner
Basic erosion processes of oxidized and clean metal cathodes by electric arcs.
IEEE Trans. Plasma Sci., Vol. PS-8(1980), p. 259-269.

[6] Poeffel, K.
Influence of the copper electrode surface on initial arc movement.
IEEE Trans. Plasma Sci., Vol. PS-8(1980), p. 443-448.

[7] Jüttner, B.
Formation time and heating mechanism of arc cathode craters in vacuum.
J. Phys. D, Vol. 14(1981), p. 1265-1275.

[8] Jüttner, B.
Cathode phenomena with arcs and breakdowns in vacuum.
Beitr. Plasma Phys., Vol. 21(1981), p. 217-232.

[9] Jüttner, B.
On the variety of cathode craters of vacuum arcs, and the influence of the cathode temperature.
Physica, Vol. 114C(1982), p. 255-261.

[10] Hantzsche, E.
The state of the theory of vacuum arc cathodes.
Beitr. Plasma Phys., Vol. 23(1983), p. 77-94.

[11] Anders, S. and B. Jüttner, H. Pursch, P. Siemroth
Investigations of the current density in the cathode spot of a vacuum arc.
Beitr. Plasma Phys., Vol. 25(1985), p. 467-473.

[12] Hantzsche, E. and B. Jüttner
Current density in arc spots.
IEEE Trans. Plasma Sci., Vol. PS-13(1985), p. 230-234.

[13] Hantzsche, E. and B. Jüttner, V.F. Puchkarov, W. Rohrbeck, H. Wolff
Erosion of metal cathodes by arcs and breakdowns in vacuum.
J. Phys. D, Vol. 9(1976), p. 1771-1781.

[14] Sherman, J.C. and R. Webster, J.E. Jenkins, R. Holmes
Cathode spot motion in high-current vacuum arcs on copper electrodes.
J. Phys. D, Vol. 8(1975), p. 696-702.

[15] Fang, D.Y.
Cathode spot velocity of vacuum arcs.
J. Phys. D, Vol. 15(1982), p. 833-844.

[16] Rakhovskii, V.I.
Experimental study of the dynamics of cathode spots developemnt.
IEEE Trans. Plasma Sci., Vol. PS-4(1976), p. 81-102.

[17] Jüttner, B. and H. Pursch, V.A. Shilov
The influence of surface roughness and surface temperature on arc spot movement in vacuum.
J. Phys. D, Vol. 17(1984), p. L31-L34.

[18] Daalder, J.E. and C.W.M. Vos
Distributionfunctions of the spotdiameter for single- and multi-cathode discharges in vacuum.
Department of Electrical Engineering, Eindhoven University of Technology, 1973. TH-Report 73-E-32.

[19] Sethuraman, S.K. and M.R. Barrault
The role of cathode surface conditions on the behaviour of vacuum arcs.
In: Proc. 7th Int. Conf. on Gas Discharges and their Applications, London, 31 Aug. - 3 Sept. 1982.
London: Peter Peregrinus, 1982. PPL Conf., No. 20. P. 47-50.

[20] Ecker, G.
Theoretical investigation of the cathode spot in a vacuum discharge.
High Temp., Vol. 16(1978), p. 1111-1119. Transl. from Teplofiz. Vys. Temp. (USSR), Vol. 16(1978), p. 1297-1304.

[21] Vacuum Arcs: Theory and application. Ed. by J.M. Lafferty.
New York: Wiley, 1980.

[22] Smeets, R.P.P.
Low-current behaviour and current chopping of vacuum arcs.
Ph.D. Thesis. Eindhoven University of Technology, 1987.

[23] Daalder, J.E.
Cathode erosion of metal vapour arcs in vacuum.
Ph.D. Thesis. Eindhoven University of Technology, 1978.

Eindhoven University of Technology Research Reports
Faculty of Electrical Engineering

ISSN 0167-9708
Coden: TEUEDE

(168) Linnartz, J.P.M.G.
SPATIAL DISTRIBUTION OF TRAFFIC IN A CELLULAR MOBILE DATA NETWORK.
EUT Report 87-E-168. 1987. ISBN 90-6144-168-4

(169) Vinck, A.J. and Pineda de Gyvez, K.A. Post
IMPLEMENTATION AND EVALUATION OF A COMBINED TEST-ERROR CORRECTION PROCEDURE FOR MEMORIES WITH DEFECTS.
EUT Report 87-E-169. 1987. ISBN 90-6144-169-2

(170) Hou Yibin
DASM: A tool for decomposition and analysis of sequential machines.
EUT Report 87-E-170. 1987. ISBN 90-6144-170-6

(171) Monnee, P. and M.H.A.J. Herben
MULTIPLE-BEAM GROUNDSTATION REFLECTOR ANTENNA SYSTEM: A preliminary study.
EUT Report 87-E-171. 1987. ISBN 90-6144-171-4

(172) Bastiaans, M.J. and A.H.M. Akkermans
ERROR REDUCTION IN TWO-DIMENSIONAL PULSE-AREA MODULATION, WITH APPLICATION TO COMPUTER-GENERATED TRANSPARENCIES.
EUT Report 87-E-172. 1987. ISBN 90-6144-172-2

(173) Zhu Yu-Cai
ON A BOUND OF THE MODELLING ERRORS OF BLACK-BOX TRANSFER FUNCTION ESTIMATES.
EUT Report 87-E-173. 1987. ISBN 90-6144-173-0

(174) Berkelaar, M.R.C.M. and J.F.M. Theeuwen
TECHNOLOGY MAPPING FROM BOOLEAN EXPRESSIONS TO STANDARD CELLS.
EUT Report 87-E-174. 1987. ISBN 90-6144-174-9

(175) Janssen, P.H.M.
FURTHER RESULTS ON THE McMILLAN DEGREE AND THE KRONECKER INDICES OF ARMA MODELS.
EUT Report 87-E-175. 1987. ISBN 90-6144-175-7

(176) Janssen, P.H.M. and P. Stoica, T. Söderström, P. Eykhoff
MODEL STRUCTURE SELECTION FOR MULTIVARIABLE SYSTEMS BY CROSS-VALIDATION METHODS.
EUT Report 87-E-176. 1987. ISBN 90-6144-176-5

(177) Stefanov, B. and A. Veefkind, L. Zarkova
ARCS IN CESIUM SEEDED NOBLE GASES RESULTING FROM A MAGNETICALLY INDUCED ELECTRIC FIELD.
EUT Report 87-E-177. 1987. ISBN 90-6144-177-3

(178) Janssen, P.H.M. and P. Stoica
ON THE EXPECTATION OF THE PRODUCT OF FOUR MATRIX-VALUED GAUSSIAN RANDOM VARIABLES.
EUT Report 87-E-178. 1987. ISBN 90-6144-178-1

(179) Lieshout, G.J.P. van and L.P.P.P. van Ginneken
GM: A gate matrix layout generator.
EUT Report 87-E-179. 1987. ISBN 90-6144-179-X

(180) Ginneken, L.P.P.P. van
GRIDLESS ROUTING FOR GENERALIZED CELL ASSEMBLIES: Report and user manual.
EUT Report 87-E-180. 1987. ISBN 90-6144-180-3

(181) Bollen, M.H.J. and P.T.M. Vaessen
FREQUENCY SPECTRA FOR ADMITTANCE AND VOLTAGE TRANSFERS MEASURED ON A THREE-PHASE POWER TRANSFORMER.
EUT Report 87-E-181. 1987. ISBN 90-6144-181-1

(182) Zhu Yu-Cai
BLACK-BOX IDENTIFICATION OF MIMO TRANSFER FUNCTIONS: Asymptotic properties of prediction error models.
EUT Report 87-E-182. 1987. ISBN 90-6144-182-X

(183) Zhu Yu-Cai
ON THE BOUNDS OF THE MODELLING ERRORS OF BLACK-BOX MIMO TRANSFER FUNCTION ESTIMATES.
EUT Report 87-E-183. 1987. ISBN 90-6144-183-8

(184) Kadete, H.
ENHANCEMENT OF HEAT TRANSFER BY CORONA WIND.
EUT Report 87-E-184. 1987. ISBN 90-6144-184-6

(185) Hermans, P.A.M. and A.M.J. Kwaks, I.V. Bruza, J. Dijk
THE IMPACT OF TELECOMMUNICATION ON RURAL AREAS IN DEVELOPING COUNTRIES.
EUT Report 87-E-185. 1987. ISBN 90-6144-185-4

(186) Fu Yanhong
THE INFLUENCE OF CONTACT SURFACE MICROSTRUCTURE ON VACUUM ARC STABILITY AND ARC VOLTAGE.
EUT Report 87-E-186. 1987. ISBN 90-6144-186-2